Dynamic Behaviour of a Rock Scour Protection Around Offshore Wind Monopile Foundations

Baelus L.,[1] and Bolle A.[1]

[1]Van Immerseelstraat 66, 2018 Antwerp, Belgium; e-mail: leen.baelus@imdc.be Corresponding author.

ABSTRACT

For the design of a rock scour protection around the monopile foundations of offshore wind farms, a static or a dynamic stability approach can be applied. The static approach allowing no movement of the rock during the design storm conditions often results in large rock sizes. A stable scour protection can still be obtained with movement of smaller rock as long as the damage does not reach the underlying filter layer. A test campaign is executed to investigate the rock movement of a scour protection for increasingly smaller rock sizes. The question is: can a dynamically stable scour protection be obtained with smaller rock sizes by increasing the armour layer thickness? The tests confirm the concept of a dynamically stable scour protection decreasing rock sizes if combined with an increasing layer thickness. This paper focusses on the influence of the armour layer thickness on the damage development of the scour protection.

INTRODUCTION

Around monopile foundations for offshore wind turbines, typically a rock scour protection is installed to protect the surrounding seabed from scouring due to waves and/or currents. For the design of this rock protection, a static or a dynamic stability approach can be applied. The static approach allowing no movement of the rock during the design storm conditions often results in large rock sizes. In order to reduce the required rock size, some movement of the rock during the design conditions can be allowed. To maintain a proper functioning of the protection however, the damage to the armour layer cannot protrude up to the filter layer. The thickness of the armour layer plays an important role in the stability of the system when movement is allowed. In this case, the design can significantly benefit from an optimum dimensioning of the layer thickness, but limited guidelines are available on this.

Chiew (1995) performed tests on an embedded scour protection with varying thicknesses and extents. The motion of the rock and the failure point of the protection are determined under unidirectional flow. The tests showed an increasing stability with increasing thickness. The effect of the layer thickness on the damage is also tested by De Vos (2008). Based on a limited number of tests with a small variation in layer thickness ($2.5D_{n50}$ versus $3.0D_{n50}$), a very small increase of the stability is found for increasing thickness but the number of tests is too limited to draw conclusions. Petersen et al. (2015) investigated the effect of the scour protection thickness on the development of edge scour of the seabed around the protection. It is observed that the thickness-

to-width ratio of the protection plays an important role on the equilibrium scour depth. The protection causes a significant disturbance of the incoming flow. As the thickness increases, it is found that the flow deviation and acceleration become stronger and the wake vortices are more developed. This results in an increase of the edge scour depth.
In order to gain more insight, a European MARINET funded series of physical flume model tests on a rock scour protection around a monopile has been carried out, subjected to combined wave and current loads. The stone sizes and layer thicknesses are varied to study their influence on the rock movement and the stability of the scour protection. Each test series is started with a static scour protection, meaning that no significant movement is expected according to Soulsby (1997) and De Vos (2012). Following, the stone size is decreased till reshaping of the rock leads to failure. Next the layer thickness is increased in order to obtain a dynamically stable scour protection. This means that reshaping of the rock occurs but due to the increased thickness exposure of the filter layer is avoided.
The tests give more insight in the dynamic behaviour of a rock protection around monopile foundations. The first analyses of the data set are discussed in De Schoesitter et al. (2014) and Whitehouse et al. (2014). In this paper the data set is examined with a focus on the armour layer thickness to gain more insight in the relation of the armour rock size and layer thickness with the behaviour of the scour protection.

EXPERIMENTAL SETUP

A series of physical model tests are carried out in a wave and current flume in the facilities of Aalborg University. The flume has a length of 21m and a width of 1.2m. Figure 1 illustrates the experimental setup in the flume. The wave flume is equipped with three twin resistance wave gauges and an acoustic doppler velocimeter (ADV). The wave gauges are installed 1.5m in front of the monopile to determine the incident waves by means of a reflection analysis. The current is measured 2m upstream of the monopile at 40% of the water depth above the bed. The scour protection is recorded during the tests by means of an underwater camera. The profile of the scour protection and the surrounding sand bed is measured underwater with a 3D profiler before, in between and after tests.
The monopile model is installed in a sand pit in the middle section of the flume. The monopile has a diameter of 0.10m, representative for a scale of 1/50. The sand pit is 2m long and covers the entire width of the flume. A thinner sand bed is extended over a total length of 5.6m. The sand bed is composed of a uniform fine sand with a median diameter of 0.169mm. At the end of the flume, an absorbing beach is installed to reduce the wave reflections below 18% at the monopile's location.
Combined waves and currents are generated, with the waves aligned with the current direction. Three different sea states are tested, corresponding with three typical storm conditions at the North Sea for shallower, intermediate and deeper areas. The hydrodynamic conditions are listed in Table 1 for the three test series. The water depth h is varied, while keeping the wave

(significant wave height H_{m0} and peak period T_p) and current (current velocity U_c) conditions constant where feasible. The waves in test series 1 are depth limited. The waves are generated with a target JONSWAP spectrum with peak enhancement factor γ of 3.3 for North Sea conditions. Each test consists of 5000 waves, split into three subtests of 1000, 2000 and 2000 waves to investigate the evolution of the damage. Hence, results are available after a total of 1000, 3000 and 5000 waves. This corresponds to a combined storm duration of approx. 3.1, 9.2 and 15.5 hours respectively in prototype.

A two-layer scour protection is installed on a flat sand bed. A granular filter layer with a medium diameter of 0.991mm and a thickness of 10mm is installed over an area with a diameter of 5 times the monopile's diameter ($5D_p$). The filter layer is covered with an armour layer extending with a slope 1:3 outside the filter layer. The rock size and the thickness of the armour layer are varied throughout the test campaign. Four different armour rock sizes are tested, with a median diameter D_{50} ranging between 2.69mm and 7.50mm. The armour layer thickness varies between 2 to 8 times D_{50}. The material characteristics are provided in Table 2.

The surface of the scour protection is profiled before the test, in between subtests after 1000 waves and after 3000 waves, as well as at the end of the test after 5000 waves. The profiler operates below the water. The measurement grid is set to 5mm by 5mm, selected for its resolution to scanning rate ratio. The vertical accuracy of the measurements is 2mm. Moreover, the armour layer is installed in coloured bands, for visual inspection of the damage. A picture of the scour protection configuration can be found in Figure 2.

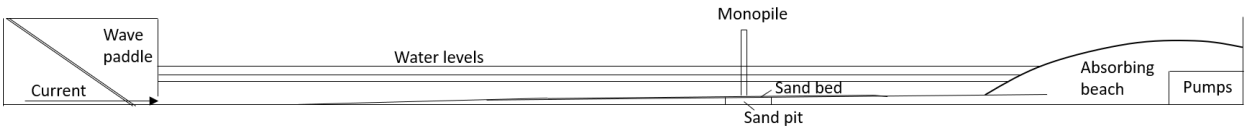

Figure 1. Experimental setup in wave and current flume (schematic profile view).

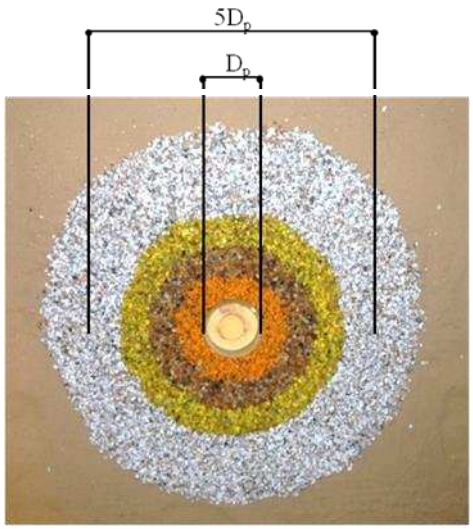

Figure 2. Scour protection configuration with colour bands (top view).

Table 1. Hydrodynamic test conditions for three sea states (model).

Test series	h [m]	H_{m0} [m]	T_p [s]	U_c [m/s]
1	0.24	0.18	0.10	1.56
2	0.36	0.18	0.14	1.56
3	0.50	0.18	0.14	1.56

Table 2. Material characteristics of scour protection and sand bed (model).

Material	D_{50} [mm]	ρ [kg/m³]
Armour 1	7.500	2650
Armour 2	6.015	2564
Armour 3	4.135	2597
Armour 4	2.686	2564
Sand	0.169	2564
Filter	0.991	2632

RESULTS OF PHYSICAL MODEL TESTS

The behaviour of the scour protection under combined wave and current loading is classified into three categories:

- Statically stable: no or limited movement of the armour rock is observed;
- Dynamically stable: movement of the armour rock is observed without failure;
- Failure: movement of the armour rock is observed exposing the filter layer over an area larger than 4 times $D_{50,armour}^2$ (den Boon et al. 2005).

Three test series are executed corresponding to the three sea states characterized in Table 1. During each test series, first the armour rock size is systematically reduced to develop from a statically stable over a dynamically stable towards a failed protection. The armour layer thickness is fixed at $2D_{50}$. Second, the armour layer thickness of the failed scour protection is systematically increased until a dynamically stable protection is found again. The results of the test series are presented in Table 3.

For most cases a dynamically stable protection is found by increasing the layer thickness after initial failure of the armour rock for a certain rock size and a layer thickness of $2D_{50}$. When the armour rock size is decreased too much, failure could no longer be avoided without exceeding a layer thickness of $8D_{50}$.

Figure 3 shows the scour and accretion pattern of the scour protection for the three damage classifications. For a statically stable test (left), limited scour is observed. Any scour is limited to the two inner rings of the protection. Accretion is found on the two outer rings of the protection, caused by sand deposits. For a dynamically stable scour protection (middle), scour occurs at the

front sides of the monopile, as well as in a V-shaped area behind the pile. Again, the scour is mainly limited to the two inner rings of the protection. Some accretion of stones is observed at the sides of the monopile in the second inner ring, as well as on the front side of the scour protection in the outer rings. This scour pattern becomes more pronounced when the test fails (right): the scour depths increase, the scour holes at the front sides enlarge and become connected at the front, and the scour hole behind the pile extents into the third ring. Significant deposition of the rock occurs along the 45° profiles from the back of the pile. The patterns are analysed in detail in De Schoesitter et al. (2014).

Table 3. Test program with damage classification of tests: statically stable (blue), dynamically stable (green) and failure (red).

Test series	Armour 1	Armour 2	Armour 3	Armour 4
1	$4D_{50}$	$2D_{50}$	$2D_{50}$	$8D_{50}$
			$3D_{50}$	
2	$2D_{50}$	$2D_{50}$	$3D_{50}$	$8D_{50}$
			$4D_{50}$	
3		$2D_{50}$	$2D_{50}$	$4D_{50}$
			$3D_{50}$	$6D_{50}$
			$4D_{50}$	$8D_{50}$

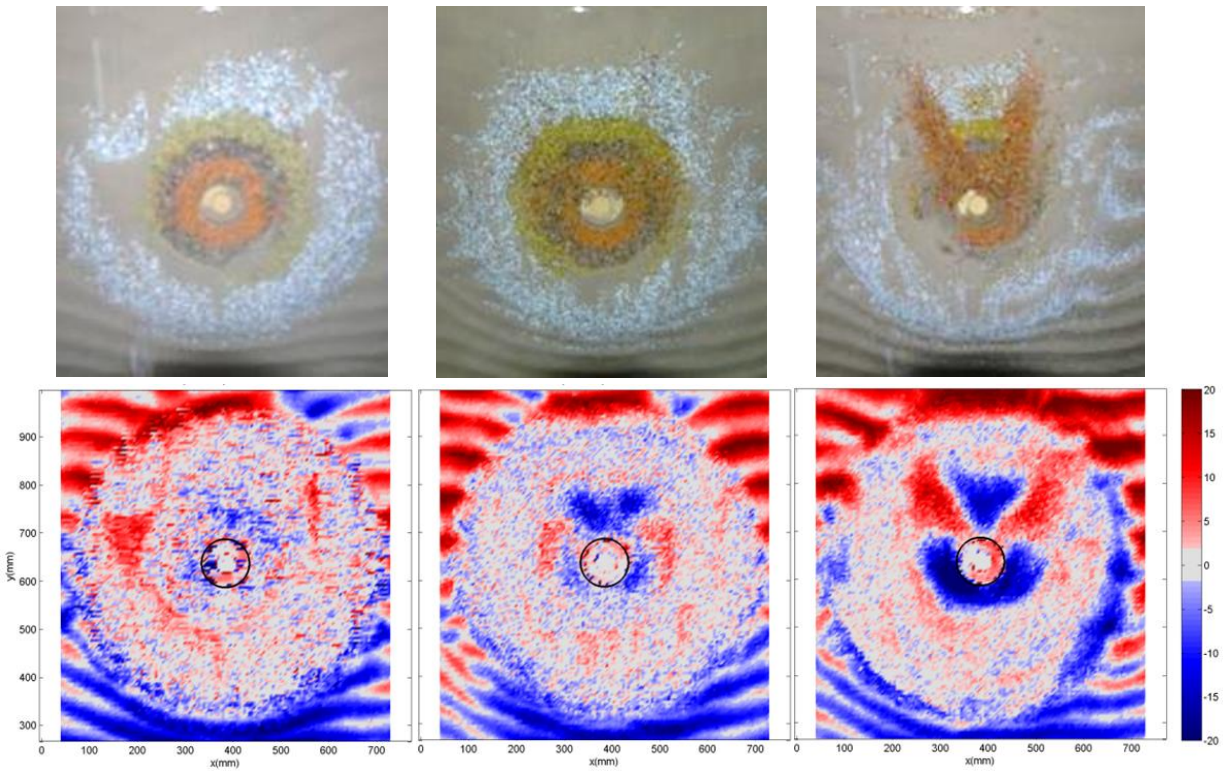

Figure 3. Scour (blue) and accretion (red) pattern of statically stable (left), dynamically stable (middle) and failed (right) scour protections in test series 2 (top view).

DAMAGE ANALYSIS

The damage is quantified using the damage number S_{3D} (De Vos 2012). The damage number represents the average eroded height over a considered area. The scour protection is divided into different subareas with an area of $\pi D_p^2/4$ whose pattern is defined taking into account a typical damage pattern (see Figure 4) and the damage number of the most eroded area is selected to be representative for the scour protection behaviour:

$$S_{3D,sub} = \frac{V_e}{D_{n50} \cdot \pi \frac{D_p^{\,2}}{4}} \quad ; \quad S_{3D} = \max_{i=1\ to\ 24}\left(S_{3D,sub,i}\right)$$

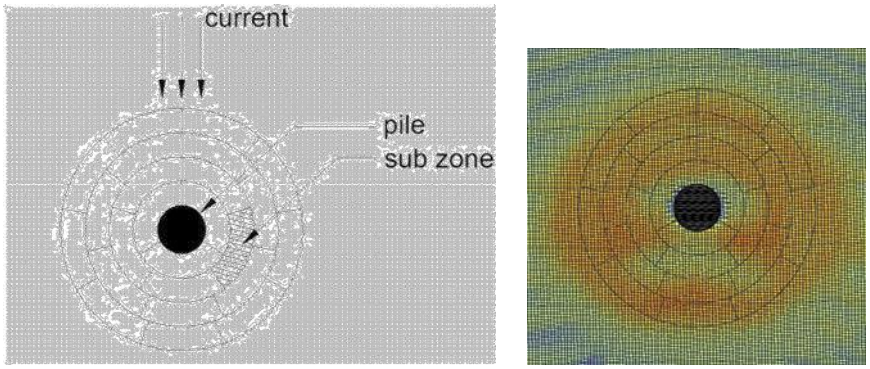

Figure 4. Division of the scour protection in different sub zones according De Vos (2012).

The measured damage number S_{3D} is plotted against the test classification from Table 3 in Figure 4 (left panel) for the data set of this paper as well as the data set of De Vos (2012). The limits of the damage number S_{3D} defined by De Vos (2012) for the different damage classifications are also included:

- Statically stable: $S_{3D} < 0.25$
- Dynamically stable: $0.25 < S_{3D} < 1.00$
- Failure: $S_{3D} > 1.00$

The use of a larger scour protection thickness obviously allows for much larger damage numbers without failure. Damage numbers up to 0.4 are measured for statically and up to 3.5 for dynamically stable tests.

The ratio of the layer thickness coefficient of De Vos (2012), i.e. 2, and the layer thickness coefficient of the data set of this paper, i.e. 2 to 8, is determined. The damage number S_{3D} is normalized to a layer thickness coefficient of 2 by multiplication with the layer thickness ratio. The normalized measured damage number S_{3D} is plotted against the test classification from Table 3 in Figure 4 (right panel). This time a reasonable correspondence of the scour protection behaviour with the threshold is found, though some exceedances of the thresholds still resulted in a stable protection.

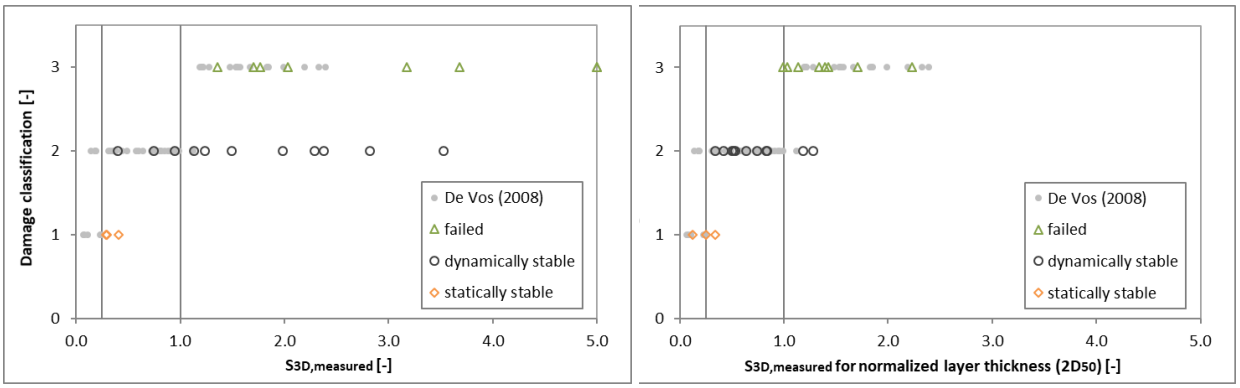

Figure 5. Damage classification versus measured damage number S_{3D} (left), normalized to an armour layer thickness of $2D_{50}$ (right).

Figure 6 (left panel) shows the damage number grouped for tests with similar hydrodynamic conditions and armour rock size, but increasing armour layer thickness. Due to the increased thickness of the scour protection, a slight increase of the hydrodynamic load on the protection is expected (Petersen et al. 2015) which could introduce a larger damage. However, the increased layer thickness results in either an increase of the damage, a status quo or even a decrease of the damage for the different comparable test sets. Certain repetition tests are performed throughout the test series, giving multiple points on the graph per layer thickness within these test sets. The scatter on the damage number of repeated tests is in most cases larger than the influence of the layer thickness on the damage number. Hence, no clear influence of the layer thickness on the damage number is found.

In Figure 6 (right panel) the damage number S_{3D} normalized for the layer thickness is used. Here a clear decrease of the normalized damage number can be observed for larger thicknesses. The increased layer thickness is decreasing the relative protrusion of the damage into the armour layer.

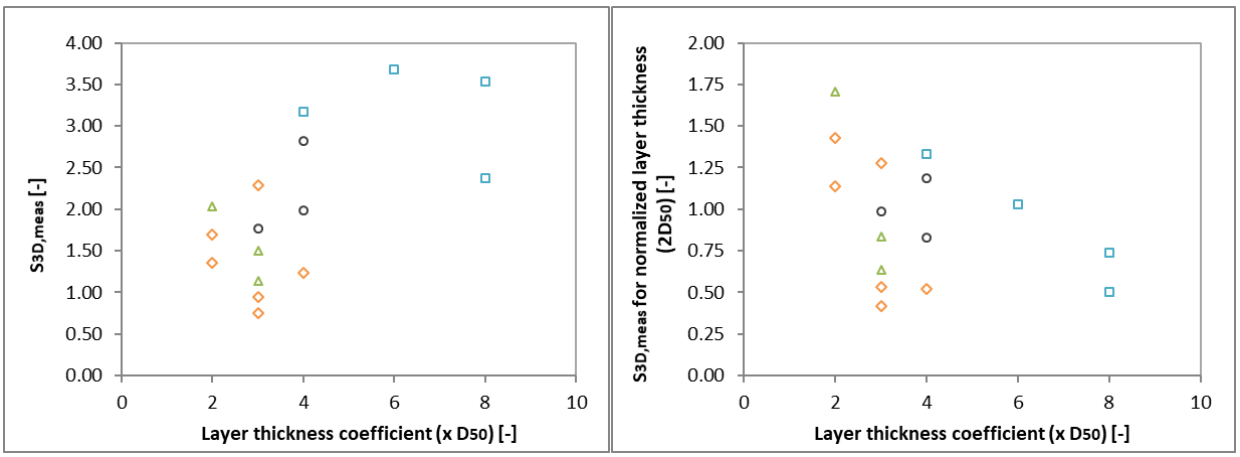

Figure 6. Influence of armour layer thickness on damage number S_{3D} (left), normalized to an armour layer thickness of $2D_{50}$ (right), for test sets with similar hydrodynamic conditions and armour rock size.

The Shields parameter θ can also be used to describe the stability of the scour protection rock. Whitehouse et al. (2014) investigated the static, dynamic and failure behaviour of the data set of the present paper by means of the Shields parameter. A clear threshold between the statically stable tests and the tests with movement or failure is found, based upon which a shear stress amplification factor of 1.8 due to the presence of the monopile is derived. This value corresponds with a stability parameter (θ_{max}/θ_{cr}) of 0.556, higher than the stability parameter derived by den Boon et al. (2005) from the OptiPile data set. Moreover, generally an increase of the stability parameter is observed for increasing layer thickness. However, no clear threshold could be observed between dynamically stable tests and failed tests.

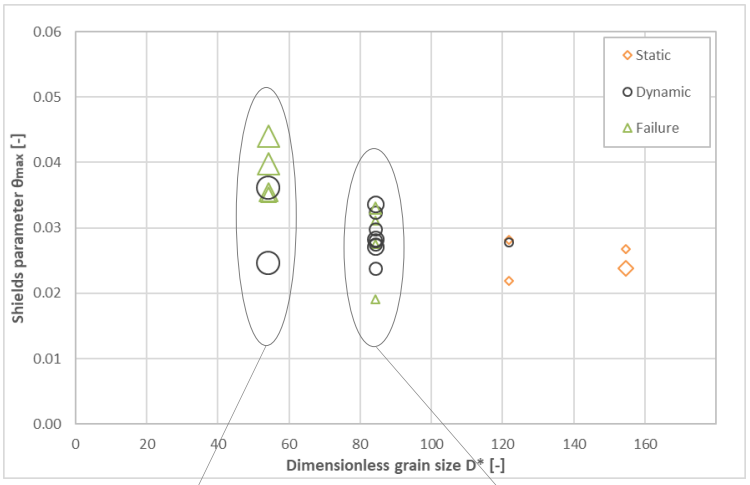

Figure 7. Shields parameter θ_{max} as a function of dimensionless grain size D* for statically stable (◊), dynamically stable (○) and failed tests (Δ).

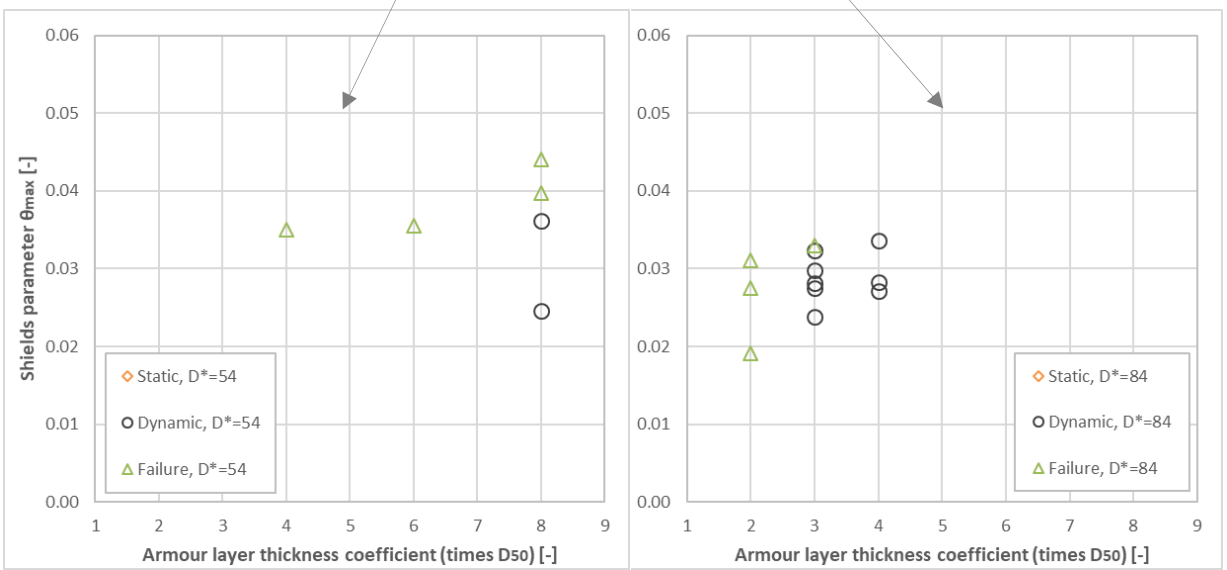

Figure 8. Shields parameter θ_{max} as a function of armour layer thickness coefficient, for statically stable (◊), dynamically stable (○) and failed tests (Δ), and for dimensionless grain size D* of 55 (left) and 84 (right).

Figure 7 shows the Shields parameter θ_{max} as a function of the dimensionless grain size D* for statically stable, dynamically stable and failed tests. This illustrated the findings of Whitehouse et al. (2014) where a threshold is defined between the statically and dynamically stable tests, but not between the dynamically stable and failed tests. The symbol size in Figure 7 is related to the armour layer thickness of the scour protection, generally showing larger Shields parameters for larger layer thickness.
Figure 8 provides more insight in this. In the data set, dynamic stability and failure are mainly observed for smaller armour rock (D* of 55 and 84). The Shields parameter θ_{max} is plotted versus the armour layer thickness coefficient, for the smallest (D*of 55, left panel) and second smallest (D* of 84, right panel) armour rock size of the test campaign. This figure shows that for similar scour protection configurations (armour rock size, armour layer thickness), the Shields parameter is always larger for failed tests than for dynamically stable tests. This shows a clear threshold from dynamically stable to failed tests, which is depending on both the influence of the layer thickness as well as the armour rock size.

CONCLUSION

The concept of a dynamically stable rock scour protection around the monopile foundation of offshore wind farms combining smaller rock sizes with increased layer thicknesses is tested in a physical model and confirmed. In a dynamically stable scour protection, movement of the rock under wave and current loads can be allowed if the damage into the armour layer does not protrude up to the filter layer. For most conditions a dynamically stable protection is found by increasing the layer thickness after initial failure of the armour rock for a certain small rock size and a layer thickness of $2D_{50}$. When the armour rock size is decreased too much, failure could no longer be avoided without exceeding a layer thickness of $8D_{50}$.
No clear relation is found between the layer thickness and the damage number S_{3D}. However, increasing the layer thickness allows for much larger damage numbers before failure of the scour protection occurs. When the damage number over layer thickness coefficient (normalized to a layer thickness of $2D_{50}$) is considered, a good correspondence with the thresholds for damage classification is observed. The increased layer thickness is decreasing the relative protrusion of the damage into the armour layer.
Using the Shields parameter θ_{max}, a significant overlap is found between the values for statically stable, dynamically stable and failed tests. It is found however that a threshold of the Shields parameter is still observed marking the transition between the different damage classifications, which is depending on both the influence of the layer thickness as well as the armour rock size.

ACKNOWLEDGEMENTS

The authors acknowledge the European Marine Renewables Infrastructure Network (MARINET) access funding, making this research possible.

The authors also kindly acknowledge the department of civil engineering of Aalborg University (AAU) for making available their hydraulic laboratory for this research.
Finally, the authors would like to thank Porto University (FEUP), Ghent University (UGent), HR Wallingford and IMDC for providing funds for this research effort.

REFERENCES

Chiew, Y.M. (1995). "Mechanics of riprap failure at bridge piers." *Journal of Hydraulic Engineering*, 121(9), 635-643.

De Schoesitter, P., Audenaert, S., Baelus, L., Bolle, A., Brown, A., das Neves, L., Ferradosa, T., Haerens, P., Taveira-Pinto, F., Troch, P., and Whitehouse, R. (2014). "Feasibility of a dynamically stable rock armour layer scour protection for offshore wind farms." *33rd International Conference on Ocean, Offshore and Arctic Engineering, OMAE 2014*, San Francisco, USA.

De Vos, L. (2008). "Optimisation of scour protection design for monopiles and quantification of wave run-up. Engineering the influence of an offshore wind turbine on local flow conditions". *PhD thesis*, Ghent University, Belgium.

De Vos, L., De Rouck, J. Troch, P., and Frigaard, P. (2012). "Empirical design of scour protections around monopile foundations. Part 2: Dynamic approach." *Coastal Engineering* 60, 286 – 298.

Den Boon, J.H., Sutherland, J., Whitehouse, R., Soulsby, R., Stam, C.J.M., Verhoven K., Høgedal, M., and Hald, T. (2005). "Scour behaviour and scour protection for monopile foundations of offshore windfarms. *Proceedings of the European Wind Energy Conference, UWEA 2004*, London, UK.

Petersen, T.U., Sumer, B.M., Fredsøe, J., Raaijmakers, T., and Schouten, J. (2015). "Edge scour at scour protection around piles in the marine environment - Laboratory and field Investigation". *Coastal Engineering* 106, 42–72.

Soulsby, R. (1997). "Dynamics of marine sands: A manual for practical applications". *Thomas Telford*, London, UK.

Whitehouse, R., Brown, A., Audenaert, S., Bolle, A., De Schoesitter, P., Haerens, P., Baelus, L., Troch, P., das Neves, L., Ferradosa, T. & Taveira-Pinto, F. (2014). "Optimising scour protection stability at offshore foundations." *7th International Conference on Scour and Erosion, ICSE7*, Perth, Australia.